

Deformed shell model results for neutrinoless double beta decay of nuclei in A=60-90 region

R. Sahu^{1*} and V.K.B. Kota^{2,3}

¹*Physics Department, Berhampur University,
Berhampur-760 007, Odisha, INDIA and*

²*Physical Research Laboratory, Ahmedabad - 380 009, INDIA*

³*Department of Physics, Laurentian University,
Sudbury, ON P3E 2C6, CANADA*

Abstract

Nuclear transition matrix elements (NTME) for the neutrinoless double beta decay of ^{70}Zn , ^{80}Se and ^{82}Se nuclei are calculated within the framework of the deformed shell model based on Hartree-Fock states. For ^{70}Zn , jj44b interaction in $^2p_{3/2}$, $^1f_{5/2}$, $^2p_{1/2}$ and $^1g_{9/2}$ space with ^{56}Ni as the core is employed. However, for ^{80}Se and ^{82}Se nuclei, a modified Kuo interaction with the above core and model space are employed. Most of our calculations in this region were performed with this effective interaction. However, jj44b interaction has been found to be better for ^{70}Zn . After ensuring that DSM gives good description of the spectroscopic properties of low-lying levels in these three nuclei considered, the NTME are calculated. The deduced half-lives with these NTME, assuming neutrino mass is 1 eV, are $9.6 \times 10^{25}\text{yr}$, $1.9 \times 10^{27}\text{yr}$ and $1.95 \times 10^{24}\text{yr}$ for ^{70}Zn , ^{80}Se and ^{82}Se , respectively.

PACS numbers: 23.40.Hc, 21.10.Tg, 21.60.Jz, 27.50.+e

*Electronic address: rankasahu@rediffmail.com

I. INTRODUCTION

Neutrinoless double beta decay ($0\nu\beta\beta$ or $0\nu DBD$) which involves emission of two electrons without the accompanying neutrinos and which violates lepton number conservation has been an important and challenging problem both for the experimentalists and theoreticians. Recent neutrino oscillation experiments have demonstrated that neutrinos have mass. The observation of $0\nu\beta\beta$ decay is expected to provide information regarding the absolute neutrino mass which is not known. To extract neutrino mass, the nuclear matrix elements must be known from a reliable nuclear model and hence the main goal of nuclear theorists is to calculate the nuclear transition matrix elements as accurately as possible. On the other hand experimental programmes have been initiated at different laboratories across the globe to observe this decay and the experiments are already in advanced stages of development. The most recent experimental results of $0\nu\beta\beta$ decay of ^{136}Xe have been reported by KamLand-Zen collaboration [1] and EXO 200 collaboration [2] and they give a lower limit of 3.4×10^{25} yr for the half-life. On the other hand, phase I results from GERDA experiment [3] for ^{76}Ge are published recently giving a lower limit of 3.0×10^{25} yr for the half-life.

Nuclear transition matrix elements (NTME) are the essential ingredient for extracting the neutrino mass from the half lives. There has been considerable effort to obtain NTME for various candidate nuclei and they have been calculated theoretically using a variety of nuclear models: (i) large scale shell model [4]; (ii) quasi-particle random phase approximation (QRPA) and its variants [5–7]; (iii) proton-neutron interacting boson model (IBM-2) [8]; (iv) particle number and angular momentum projection including configuration mixing within the generating coordinate method framework (GCM+PNAMP) [9]; (v) projected Hartree-Fock-Bogoliubov (PHFB) method with pairing plus quadrupole quadrupole interaction [10]. Detailed comparative study of the results from these methods is discussed recently in [11].

Besides the two electron mode, it is also possible to have neutrinoless positron double beta decay and this can come in three modes: (i) double β^+ ($\beta^+\beta^+$), (ii) β^+ and electron capture ($\beta^+\text{EC}$) and (iii) double electron capture (ECEC). All these three modes combined are referred to as $0\nu e^+DBD$. There are now efforts to observe 0ν (and also 2ν) e^+DBD in some nuclei; see for example [12–14].

Over the last many years, the Deformed Shell Model (DSM) (based on Hartree-Fock states) has been used to study various properties of nuclei in the mass $A=60$ -90 region (also

in A=44-60) with reasonable success. They include: (i) spectroscopic properties such as band structures, shapes and shape coexistence, nature of band crossings, electromagnetic transition probabilities [15–20]; (ii) $T = 1$ and $T = 0$ bands in N=Z odd-odd nuclei and $T = 1/2$ bands in odd-A nuclei by including isospin projection [21–23]; (iii) transition matrix elements for $\mu - e$ conversion in ^{72}Ge [24] and in the analysis of data for inelastic scattering of electrons from fp -shell nuclei [25]. More importantly, this model has also been used for studying 2ν double beta decay, in a first attempt, for $^{76}\text{Ge} \rightarrow ^{76}\text{Se}$ in [26] with reasonable success. Following this and the success of DSM in explaining spectroscopic properties of nuclei in A=60-90 region, we have started a study of DBD in A=60-90 nuclei.

As shown in table I, there are eight candidate nuclei in the A=60-90 region with $30 \leq Z \leq 40$ and $N \leq 48$ which can undergo double beta decay. We have already applied DSM to study half lives for 2ν e^+ DBD in ^{78}Kr [27], in ^{74}Se [28], in ^{84}Sr [29] and in ^{64}Zn [30]. Going further, more recently we have also calculated NTME for neutrinoless positron double beta decay $0\nu\beta^+\beta^+$ and $0\nu\beta^+\text{EC}$ for all the above four nuclei [30]. We ensured that DSM gives a good description of the spectroscopic properties for low-lying states for these nuclei. The deduced half-lives with these NTME, assuming neutrino mass is 1 eV, are smallest for ^{78}Kr with half life for $\beta^+\text{EC}$ decay being $\sim 10^{27}$ yr. For all others, the half lives are in the range of $\sim 10^{28}$ to 10^{29} yr.

TABLE I: DBD candidates with A=60-90, $30 \leq Z \leq 40$ and $N \leq 48$.

$(0 + 2\nu)\beta^-\beta^-$	$(0 + 2\nu)e^+\text{DBD}$
^{70}Zn	^{64}Zn
^{76}Ge	^{74}Se
^{80}Se	^{78}Kr
^{82}Se	^{84}Sr

In addition to completing the study of the four candidate nuclei listed in Table I that undergo e^+ DBD, in [30] we have also reported DSM results for 0ν DBD for ^{76}Ge . With this, we are left with the analysis of 2ν and 0ν DBD in ^{70}Zn , ^{80}Se and ^{82}Se nuclei (first DSM results for 2ν DBD for ^{82}Se were given in [31]). Our purpose in the present paper is to present DSM results for these nuclei. We will give a preview.

In Section 2 discussed briefly are the formula for half life for 0ν DBD, the transition

operator generating NTME and the DSM model. Section 3 gives DSM results for ^{70}Zn first for spectroscopic properties and then the results for both 2ν and 0ν double beta decay half lives. In Section 4, DSM results for 2ν and 0ν double beta decay half lives for ^{80}Se are given and similarly in Section 5 for ^{82}Se . Not many theoretical calculations of spectroscopic properties of ^{70}Zn are available in the literature. Our results obtained using DSM are presented in Section 3. Also, DSM results for orbit occupancies for all the three nuclei are discussed in Sections 3-5. Finally, Section 6 gives conclusions.

II. FORMALISM

A. $0\nu\text{DBD}$ half life and transition operator

Half-life for $0\nu\text{DBD}$ for the 0_i^+ ground state (gs) of a initial even-even nucleus decaying to the 0_f^+ gs of the final even-even nucleus is given by [11]

$$[T_{1/2}^{k:0\nu}(0_i^+ \rightarrow 0_f^+)]^{-1} = G^{0\nu}(k) (g_A)^4 |M^{0\nu}(0^+)|^2 \left(\frac{\langle m_\nu \rangle}{m_e} \right)^2, \quad (1)$$

where $\langle m_\nu \rangle$ is the effective neutrino mass (a combination of neutrino mass eigenvalues and it also involves neutrino mixing matrix) and k denotes the decay modes. The $G^{0\nu}(k)$ is phase space integral (kinematical factor) dependent on charge, mass and available energy for the $0\nu\text{DBD}$ process. In Eq. (1), the $M^{0\nu}$ is the nuclear transition matrix element (NTME) of the $0\nu\text{DBD}$ transition operator and it is a sum of a Gamow-Teller like (M_{GT}), Fermi like (M_F) and tensor (M_T) two-body operators. As it is well known that the tensor part contributes only up to 10% of the matrix elements [11], we will neglect the tensor part. Then we have, from the closure approximation which is well justified for $0\nu\text{DBD}$,

$$\begin{aligned} M^{0\nu}(0^+) &= M_{GT}^{0\nu}(0^+) - \frac{g_V^2}{g_A^2} M_F^{0\nu}(0^+) = \langle 0_f^+ || \mathcal{O}(2:0\nu) || 0_i^+ \rangle, \\ \mathcal{O}(2:0\nu) &= \sum_{a,b} \mathcal{H}(r_{ab}, \bar{E}) \tau_a^+ \tau_b^+ \left(\sigma_a \cdot \sigma_b - \frac{g_V^2}{g_A^2} \right). \end{aligned} \quad (2)$$

Note that τ^+ changes a neutron into a proton. As seen from Eq. (2), $0\nu\text{DBD}$ half-lives are generated by the two-body transition operator $\mathcal{O}(2:0\nu)$; note that a, b label nucleons. The g_A and g_V are the weak axial-vector and vector coupling constants. The $\mathcal{H}(r_{ab}, \bar{E})$ in Eq. (2) is the ‘neutrino potential’. Here \bar{E} is the average energy of the virtual intermediate states used in the closure approximation [11, 32–35]. The form given by Eq. (2) is justified *only*

if the exchange of the light Majorana neutrino is indeed the mechanism responsible for the $0\nu DBD$. The effects of short-range correlations in the wave functions are taken into account by multiplying the wave function by the Jastrow function $[1 - \gamma_3 e^{-\gamma_1 r_{ab}^2} (1 - \gamma_2 r_{ab}^2)]$ [33, 35]. Now keeping the wave functions unaltered, the Jastrow function can be incorporated into $\mathcal{H}(r_{ab}, \overline{E})$ giving an effective $\mathcal{H}_{eff}(r_{ab}, \overline{E})$,

$$\mathcal{H}(r_{ab}, \overline{E}) \rightarrow \mathcal{H}_{eff}(r_{ab}, \overline{E}) = \mathcal{H}(r_{ab}, \overline{E}) [1 - \gamma_3 e^{-\gamma_1 r_{ab}^2} (1 - \gamma_2 r_{ab}^2)]^2. \quad (3)$$

The values chosen for the parameters γ_1 , γ_2 and γ_3 are given below. For further details regarding the transition operator, see [30].

There are a number of parameters in the $0\nu DBD$ transition operator and the choices made for the various parameters are: (i) $R = 1.2A^{1/3}$ fm; (ii) $b = 1.003A^{1/6}$ fm [11]; (iii) $\overline{E} = 1.12A^{1/2}$ MeV [34]; (iv) $g_A/g_V = 1$ (quenched); (v) $(\gamma_1, \gamma_2, \gamma_3)$ in Eq. (3) are (1.1, 0.68, 1) [Miller-Spencer] [35, 36]. Now we will discuss briefly the deformed shell model formulation for calculating NTME.

B. DSM model

In DSM, for a given nucleus, starting with a model space consisting of a given set of single particle (sp) orbitals and effective two-body Hamiltonian, the lowest energy intrinsic states are obtained by solving the Hartree-Fock (HF) single particle equation self-consistently. Excited intrinsic configurations are obtained by making particle-hole excitations over the lowest intrinsic state. These intrinsic states $\chi_K(\eta)$ do not have definite angular momenta. and states of good angular momentum projected from an intrinsic state $\chi_K(\eta)$ can be written in the form

$$\psi_{MK}^J(\eta) = \frac{2J+1}{8\pi^2\sqrt{N_{JK}}} \int d\Omega D_{MK}^{J*}(\Omega) R(\Omega) |\chi_K(\eta)\rangle \quad (4)$$

where N_{JK} is the normalization constant given by

$$N_{JK} = \frac{2J+1}{2} \int_0^\pi d\beta \sin \beta d_{KK}^J(\beta) \langle \chi_K(\eta) | e^{-i\beta J_y} | \chi_K(\eta) \rangle. \quad (5)$$

In Eq. (4) Ω represents the Euler angles (α, β, γ) , $R(\Omega)$ which is equal to $\exp(-i\alpha J_z)\exp(-i\beta J_y)\exp(-i\gamma J_z)$ represents the general rotation operator. The good angular momentum states projected from different intrinsic states are not in general orthogonal

to each other. Hence they are orthonormalized and then band mixing calculations are performed. For details see [30].

DSM is well established to be a successful model for transitional nuclei (with $A=60-90$) when sufficiently large number of intrinsic states are included in the band mixing calculations. Performing DSM calculations for the parent and daughter and then using the DSM wave functions, the $\mathcal{O}(2 : 0\nu)$ operator matrix elements are calculated and the results are presented in the next three Sections.

III. ^{70}Zn RESULTS

A. Spectroscopic properties

The double beta decay of ^{70}Zn has recently been studied experimentally by Belli et al [12] (they set the lower limits to the half life for neutrinoless DBD to be $3.2 \times 10^{19}\text{yr}$ at 90% C.L.). Its natural isotopic abundance is 0.62%. Before going to double beta decay, we will first study its spectroscopic properties using DSM model to test the goodness of the model for this nucleus.

^{70}Zn with 30 protons and 40 neutrons lie near the proton shell closure and neutron subshell closure. The daughter nucleus ^{70}Ge has two neutrons less and two protons more. The ground state energy spectra for both the nuclei are similar. The energy levels are more or less equispaced. As discussed in Sect. II.B., we first carry out an axially symmetric HF calculation for each nucleus using the newly developed jj44b effective interaction [37] within the model space consisting of the orbitals $^2p_{3/2}$, $^1f_{5/2}$, $^2p_{1/2}$ and $^1g_{9/2}$ with ^{56}Ni as the core. The spherical single particle energies for these orbits are taken as -9.6566, -9.2859, -8.2695 and -5.8944 MeV and are kept same both for protons as well as neutrons. In the past we have performed many calculations in this region using a modified Kuo interaction. However, ^{70}Zn lies very close to the proton shell closure and the modified Kuo interaction has been found to be inadequate for this nucleus. Hence we study this nucleus using the jj44b effective interaction developed by Brown and his group [37]. The lowest energy HF solutions for ^{70}Zn and its daughter nucleus ^{70}Ge are shown in Fig. 1. The two active protons in ^{70}Zn occupy the lowest $k = 1/2^-$ orbital. There is a well defined gap of 3.7 MeV above the proton Fermi surface. The neutron gap above the neutron Fermi surface is 1.3 MeV. As a result, ^{70}Zn

has relatively stable deformation in the ground state. As discussed before, particle-hole excitations over the lowest HF solution are carried out and generated a total of 226 intrinsic states (with $K = 0^+$ and $K \neq 0^+$ up to 6 MeV excitation). Angular momentum projection from each of these intrinsic states is carried out and then a band mixing calculation is performed. The calculated levels are classified on the basis of their B(E2) values and also the structure of the levels.

The single particle spectrum for the lowest energy HF solution for the daughter nucleus ^{70}Ge is also shown in figure 1. The proton and neutron gaps above their respective Fermi surfaces are less than 1 MeV. Hence one can easily excite protons and neutrons above their Fermi surfaces. We have considered 180 configurations with $K = 0^+$ and $K \neq 0^+$ up to 6 MeV excitation. Good angular momentum states are projected from each of these intrinsic states and then a band mixing calculation is performed to orthonormalize these projected states. The calculated levels having similar structure and connected by relatively large B(E2) are classified as belonging to one band.

The calculated levels and the bands for ^{70}Zn and ^{70}Ge are compared with experiment in Figs. 2 and 3. The experiment data for the two nuclei are taken from [38]. The calculated spectrum is slightly compressed compared to experiment. Except for the $2^+ \rightarrow 0^+$ separation, the relative spacing of all the other levels are reasonably reproduced. The ground band in both nuclei is mainly an admixture of the lowest intrinsic configuration at low spin. However at higher spins, there is mixing due to other configurations. The quasi-gamma band is also reasonably well reproduced in both the nuclei. The quantities near the arrows represent B(E2) values in W.u. unit. The agreement with experiment for the B(E2) values is quite satisfactory. The B(E2) values are calculated with effective charges of $e_p=1.5$ and $e_n=0.5$. The B(E2) values provide a test of the goodness of nuclear wave functions generated in the model. In view of the good agreement, we have confidence about the suitability of the model for studying double beta decay properties.

Going beyond these, orbit occupancies for protons and neutron for these nuclei are presented in fig. 4. It is important to add that, recently there has been experimental efforts to measure the population of the valence orbits in several double beta decay candidate nuclei [39–43]. It will be quite useful if single nucleon transfer experiments are performed for ^{70}Zn and ^{70}Ge nuclei to test these results.

B. 2ν DBD half lives and 0ν DBD NTME and half lives

First we will consider 2ν DBD and the half-life for the $0_I^+ \rightarrow 0_F^+$ double beta decay is given by [44]

$$[T_{1/2}^{2\nu}]^{-1} = G_{2\nu} |M_{2\nu}|^2 \quad (6)$$

The kinematical factor $G_{2\nu}$ is independent of nuclear structure and its value $G_{2\nu} = 0.32 \times 10^{-21} \text{ yr}^{-1}$ [44]). On the other hand, the nuclear transition matrix elements (NTME) $M_{2\nu}$ are nuclear model dependent and they are given by,

$$M_{2\nu} = \sum_N \frac{\langle 0_F^+ || \sigma \tau^+ || 1_N^+ \rangle \langle 1_N^+ || \sigma \tau^+ || 0_I^+ \rangle}{[E_N - (E_I + E_F)/2] / m_e} \quad (7)$$

where $|0_I^+\rangle$, $|0_F^+\rangle$ and $|1_N^+\rangle$ are the initial, final and virtual intermediate states respectively and E_N are the energies of the intermediate nucleus ^{70}Ga . Similarly E_I and E_F are the ground state energies of the parent and daughter nuclei. We have from [45], the atomic masses of ^{70}Zn , ^{70}Ga and ^{70}Ge to be -69.5646 , -68.9101 and -70.5631 MeV respectively (for nuclear mass, we need to subtract the mass of the electrons from the atomic mass). For ^{70}Ga , 1^+ is the ground state. Then, with E_{1+} denoting the relative energies of the 1^+ states in ^{70}Ga with respect to the lowest 1^+ state, we finally obtain $[E_N - (E_I + E_F)/2] = [1.1537 + E_{1+}]$ MeV. DSM is used to calculate E_{1+} .

In the DSM calculations we have considered 30 lowest intrinsic states with $K = 0^+$ for ^{70}Zn , 26 lowest intrinsic configurations with $K = 0^+$ for the daughter nucleus ^{70}Ge and 65 intrinsic states with $K = 1^+$ or $K = 0^+$ for the intermediate nucleus ^{70}Ga . The intrinsic states with $K = 1^+$ or $K = 0^+$ for ^{70}Ga are generated by making particle-hole excitations over the lowest HF intrinsic state generated for this nucleus. We project out 1^+ states from each of these intrinsic states and then perform a band mixing calculation as discussed above. Taking the phase space factor $0.32 \times 10^{-21} \text{ yr}^{-1}$ [44] the DSM value for the 2ν DBD half-life is 3.39×10^{23} . Bobyk et al [46] have evaluated the half life for the $2\nu\beta\beta$ decay using different variants of QRPA with different values of g_{ph} and g_{pp} and their value varies from 5×10^{20} to 6.4×10^{23} . Our calculated half life lies near the value in the upper limit.

Spectroscopic results and $2\nu\text{DBD}$ half lives show that we can use DSM for reliable predictions for 0ν DBD. Turning to this, in the calculation of half-lives for 0ν DBD we have considered 30 intrinsic states with $K = 0^+$ for ^{70}Zn and 26 intrinsic configurations with $K = 0^+$ for the daughter nucleus ^{70}Ge as in 2ν case. The calculated NTME comes out to

be 0.71. As discussed in detail in our earlier publication [30], DSM results for NTME need to be normalized by a factor 3. This is a result of the fact that DSM is an approximation to the spherical shell model. The NTME obtained using DSM for ^{76}Ge are compared with large shell model results [4] to arrive at the renormalization factor. Thus, the NTME for ^{70}Zn is 2.13. Now, using Eq. (1), taking the neutrino mass to be 1 eV and the phase space factor $0.23 \times 10^{-26} \text{ yr}^{-1}$ from [44], the calculated half-life for $0\nu\beta\beta$ decay is $9.6 \times 10^{25} \text{ yr}$ (note that in [44], the factors $(g_A)^4$ and $(m_e)^2$ appearing in Eq. (1) are absorbed in the phase space factor $G^{0\nu}$). At present very low lower bounds ($\geq 3.2 \times 10^{19} \text{ yr}$ at 90% C.L.) for the 0ν DBB half life for ^{70}Zn is known from experiments [12]. The half-lives are displayed in table III.

IV. ^{80}Se RESULTS

A. Spectroscopic properties

In the double beta decay of ^{80}Se , the daughter nucleus is ^{80}Kr . As in the case of ^{70}Zn , we will first consider spectroscopic properties of these nuclei before discussing the double beta decay results. Both the nuclei are studied using the modified Kuo effective interaction given in [47] in the model space consisting of the single particle orbitals $^2p_{3/2}$, $^1f_{5/2}$, $^2p_{1/2}$ and $^1g_{9/2}$ with ^{56}Ni as the core. This effective interaction was used by us in most of our calculations for $A=60-90$ nuclei. The spherical single particle energies for these orbitals are taken as 0.0, 0.78, 1.08 and 4.25 MeV for protons and 0.0, 0.78, 1.58 and 2.75 MeV for neutrons. It may be mentioned that we had performed a preliminary study of the spectroscopy of ^{80}Kr and ^{82}Kr [48] with spherical single particle energies of neutrons to be same as protons taken above. However the present set of single particle energies gives much better description of spectroscopic properties. The HF single particle spectrum for these two nuclei are given in Fig. 5. For ^{80}Se , there is a well defined gap of 2.3 MeV above the proton Fermi surface and the gap above the neutron Fermi surface is 1.2 MeV. Thus, ^{80}Se has a relatively stable space. On the other hand, for ^{80}Kr , the proton and neutron gaps above their respective Fermi surfaces are much smaller. For studying spectroscopic properties of ^{80}Se , we have considered 10 intrinsic states (including the lowest one). The excited configurations are obtained by making particle-hole excitations over the lowest configuration. As discussed

above, good angular momentum states are projected from each of these intrinsic states and then these good J states are orthonormalized. The calculated spectrum is compared with experiment in fig. 6. The agreement is quite satisfactory for the ground band. The $B(E2)$ values are given near the arrows in the figure and the known $B(E2)$ s are well reproduced. In order to study the energy spectrum of the daughter nucleus ^{80}Kr , we have considered a total of 12 intrinsic states, the excited ones are obtained by particle-hole excitation. The energy spectrum obtained after angular momentum projection and band mixing is shown in fig. 7. Experimentally for this nucleus, the ground band up to $J = 10^+$ and a quasi-gamma band have been observed. This nucleus shows three 8^+ and two 10^+ levels. The ground band and the quasi-gamma band are quite well reproduced in our calculation. We find that a proton aligned band crosses the ground band at $J = 10^+$. In addition, we predict an excited $K = 0^+$ band. In our calculation, we also obtain three close lying 8^+ and two close lying 10^+ levels as in the experiment. We have calculated $B(E2)$ values for all possible transitions. The comparison with experiment for some of the $B(E2)$ values are given in Table II. In the calculation of $B(E2)$, we have used the effective charges 1.6 and 1.0 for protons and neutrons as in our earlier calculations with this effective interaction. For both the nuclei, we have also calculated the orbit occupancies and they are displayed in Fig. 4.

B. 2ν DBD half lives and 0ν DBD NTME and half lives

The $2\nu\beta\beta$ decay for this nucleus is studied using the Eqns. 6 and 7. The atomic masses of ^{80}Se , ^{80}Kr and the intermediate nucleus ^{80}Br are -77.7599, -77.8925 and -75.8895 MeV respectively as given in [45]. For the intermediate nucleus ^{80}Br , 1^+ is the ground state. Taking E_{1+} to be the calculated energies of ^{80}Br with respect to the lowest 1^+ , the energy denominator is given by $[E_N - (E_I + E_F)/2] = [1.9367 + E_{1+}]$ MeV. DSM is used to calculate E_{1+} . In the DSM calculation for $2\nu\beta\beta$, we have considered 13 configurations for ^{80}Se , 55 configurations for the daughter nucleus ^{80}Kr , all with $K = 0^+$. For the intermediate nucleus ^{80}Br , we considered 99 configurations with $K = 1^+$ or $K = 0^+$. For the odd-odd nucleus like ^{80}Br , the configurations with $K = 0^+$ can also give 1^+ levels. We project out 0^+ levels for the parent and daughter nuclei and then orthonormalize them separately. Similarly, for the intermediate nucleus ^{80}Br , we project out 1^+ levels from all the configurations and then orthonormalize them. The calculated half life with phase space factor 0.12×10^{-27} [44] comes

out to be 1.97×10^{29} yr. This value agrees quite well with the QRPA result quoted by Bobyk et al. [46]

Then we proceed to calculate the nuclear matrix element for neutrinoless double beta decay. As above we considered 13 configurations for the parent nucleus ^{80}Se and 55 intrinsic states for the daughter nucleus ^{80}Kr . The $0\nu\beta\beta$ nuclear matrix element, with the factor 3 mentioned in Section III, comes out to be 3.48. Then taking the neutrino mass to be 1 eV and phase space factor $0.43 \times 10^{-28} \text{ yr}^{-1}$ [44], the half-life is 1.9×10^{27} yr. The half-lives are displayed in table III.

V. ^{82}Se RESULTS

A. Spectroscopic properties

As in the case of ^{80}Se , we perform the calculation of ^{82}Se and the daughter nucleus ^{82}Kr using the modified Kuo effective interaction in the model space consisting of the single particle orbitals $^2p_{3/2}$, $^1f_{5/2}$, $^2p_{1/2}$ and $^1g_{9/2}$ with ^{56}Ni as the core. The spherical single particle energies for these orbitals are taken as 0.0, 0.78, 1.08 and 4.25 MeV for protons and 0.0, 0.78, 1.58 and 2.75 MeV for neutrons. As before, we first perform axially symmetric HF calculation for both the nuclei and obtain the lowest energy prolate solution. The lowest energy prolate solution is shown in Fig. 8. ^{82}Se also has a well defined gap 2.1 MeV and 3.2 MeV above the proton and neutron Fermi surfaces and hence it has a stable shape. However for the daughter nucleus ^{82}Kr , the gaps are much smaller. The proton gap is only 0.9 MeV whereas the neutron gap is 1.8 MeV. For calculating the energy spectrum, we perform particle-hole excitations over the lowest HF configuration for each nucleus and obtain excited intrinsic states. Good angular momentum states are projected from each of these intrinsic states. These good angular momentum states are then orthonormalized and then a band mixing calculation is performed. For studying the energy spectrum of ^{82}Se , we considered 10 intrinsic states. The energy spectrum is given in fig. 9. The ground band is quite well reproduced in our calculation. We find that a neutron aligned band crosses the ground band at $J = 8^+$. Recently we had studied the $2\nu\beta\beta$ decay of this nucleus [31] using a slightly different set of spherical single particle energies. The energy spectrum is more or less similar to the present case. We have calculated $B(E2)$ values for all possible transitions

taking effective charges 1.6 and 1.0 for protons and neutrons. In the ground band, only two B(E2) transitions are known and they are in good agreement with DSM values as shown in Fig. 9.

For calculating the spectroscopic properties of the daughter nucleus ^{82}Kr , we have considered 12 intrinsic states. After angular momentum projection and orthonormalization, the energy bands obtained in our calculation are compared in Fig. 10. The ground band and the quasi-gamma band are quite nicely reproduced in our calculation. We calculate the B(E2) values with the same effective charges as in ^{80}Se . The B(E2) values are compared with experiment in Table II. The agreement is quite satisfactory.

B. 2ν DBD half lives and 0ν DBD NTME and half lives

The two 2ν DBD for ^{82}Se is first studied using Eqns. 6 and 7. We have considered 7 intrinsic states for ^{82}Se and 48 intrinsic states for the daughter nucleus ^{80}Kr all with $K = 0^+$. $J = 0^+$ states are projected out from each of these intrinsic states and then these states are orthonormalized for each nucleus. The intermediate nucleus ^{82}Br generates the 1^+ states. Excited configurations with $K = 0^+$ and $K = 1^+$ for the intermediate nucleus are obtained by making particle-hole excitations over the lowest HF intrinsic configuration. Then we perform angular momentum projection to project out $J = 1^+$ levels from each intrinsic state. These angular momentum states are then orthonormalized. We took 83 configurations with $K = 0^+$ or $K = 1^+$ and calculated the numerator of Eq. (7). The atomic masses for the parent, intermediate and daughter nuclei are -77.5940, -77.4965 and -80.5895 MeV respectively [45]. For this nucleus, the lowest 1^+ state is at an excitation of 0.075 MeV. If E_{1+} are the energies of the excited 1^+ states with respect to the lowest one which are calculated within our DSM model, the energy denominator is given by $(1.6702 + E_{1+})$. With the phase space factor $0.43 \times 10^{-17} \text{ yr}^{-1}$ [44], we predict the half life to be $1.58 \times 10^{19} \text{ yr}$ compared to the experimental value $(0.92 \pm 0.07) \times 10^{20} \text{ yr}$.

Then we proceed to calculate the neutrinoless double beta decay half life. We take 7 configurations for the parent nucleus ^{82}Se and 48 configurations for the daughter nucleus ^{82}Kr as in the two neutrino case with $K = 0^+$. Good $J = 0^+$ states are projected from these intrinsic states and they are orthonormalized by performing band mixing calculation for each nucleus. The calculated nuclear matrix element, with renormalization, is 2.16. Taking

the phase space factor $0.11 \times 10^{-24} \text{ yr}^{-1}$ [44] and the neutrino mass to be 1eV, the half life is $1.95 \times 10^{24} \text{ yr}$. The half lives are presented in table III. It should be added that there is considerable interest in ^{82}Se because of the upcoming SuperNEMO experiment [49]. The NEMO-3 gave a lower limit of $3.2 \times 10^{23} \text{ yr}$ at 90% C.L. for this nucleus [49]. With SuperNEMO coming soon, new large scale shell model calculations are being carried out and the current values for NTME from shell model are $\sim 3 - 3.4$ [50].

VI. CONCLUSIONS

In the $A=60-90$ region with $30 \leq Z \leq 40$ and $N \leq 48$ there are eight candidate nuclei, as shown in Table I, which can undergo double beta decay. Prompted by the success of deformed shell model, based on Hartree-Fock intrinsic states with band mixing, in explaining spectroscopic properties of nuclei in the $A=60-90$ region, recently DSM results for the four $0\nu e^+ \text{DBD}$ candidate nuclei, i.e. ^{64}Zn , ^{74}Se , ^{78}Kr and ^{84}Sr have been reported by us in [30]. Similarly the results for $2\nu e^+ \text{DBD}$ half lives are reported in [27–30]. In addition, results for 2ν and $0\nu \text{DBD}$ for ^{76}Ge have been reported in [26] and [30] respectively. Complementing this work, in the present paper DSM results for $0\nu \text{DBD}$ for the three remaining nuclei, i.e. for ^{70}Zn , ^{80}Se and ^{82}Se are presented. After ensuring reasonable DSM description of spectroscopic properties that include spectra and $B(E2)$'s, we have presented the results for occupancies for the parent and daughter nuclei involved. Proceeding further, DSM results for NTME and there by for the $0\nu \text{DBD}$ half-lives are presented for ^{70}Zn , ^{80}Se and ^{82}Se as shown in Table III. The present paper brings to conclusion DSM study of the eight DBD candidate nuclei listed in Table I. Future DSM studies call for using much larger set of single particle levels, suitable effective interactions in the larger spaces and inclusion of much larger number of intrinsic states in band mixing calculations.

Acknowledgments

RS is thankful to DST (Government of India) for financial support. RS and VKBK thank

H.J. Kim, KNU, South Korea for his interest in the present work.

- [1] A. Gando *et al.*, Phys. Rev. Lett. **110**, 062502 (2013).
- [2] M. Auger *et al.*, Phys. Rev. Lett. **109**, 032505 (2012).
- [3] M. Agostini *et al.*, Phys. Rev. Lett. **111**, 122503 (2013).
- [4] E. Caurier, J. Menéndez, F. Nowacki, and A. Poves, Phys. Rev. Lett. **100**, 052503 (2008)
- [5] F. Šimkovic, A. Faessler, V. Rodin, P. Vogel and J. Engel, Phys. Rev. C **77**, 045503 (2008)
- [6] D.-L. Fang, A. Faessler, V. Rodin and F.Šimkovic, Phys. Rev. C **83**, 034320 (2011)
- [7] M. Kortelainen and J. Suhonen, Phys. Rev. C **75**, 051303(R) (2007).
- [8] J. Barea, J. Kotila, and F. Iachello, Phys. Rev. Lett. **109**, 042501 (2012).
- [9] T.R. Rodríguez and G. Martinez-Pinedo, Phys. Rev. Lett. **105**, 252503 (2010)
- [10] K. Chaturvedi, R. Chandra, P.K. Rath, P.K. Raina, and J.G. Hirsch, Phys. Rev. C **78**, 054302 (2008)
- [11] J. Barea, J. Kotila, and F. Iachello, Phys. Rev. C **87**, 014315 (2013).
- [12] B P. Belli *et al.*, J. Phys. G: Nucl. Part. Phys. **38**, 115107 (2011).
- [13] A.S. Barabash, P. Hubert, A. Nachab, and V. Umatov, Nucl. Phys. A **785**, 371 (2007).
- [14] http://www.apctp.org/topical/2009/npap2009/Presentations/APCTP_NPAP2009_192_Kim.pdf
- [15] R. Sahu and S.P. Pandya, J. Phys. G **14**, L165 (1988).
- [16] R. Sahu and S.P. Pandya, Nucl. Phys. **A548**, 64 (1992).
- [17] K.C. Tripathy and R. Sahu, J. Phys. G **20**, 911 (1994).
- [18] R. Sahu and S.P. Pandya, Nucl. Phys. **A571**, 253 (1994).
- [19] K. C. Tripathy and R. Sahu, Nucl. Phys. **A597**, 177 (1996).
- [20] K.C. Tripathy and R. Sahu, Int. J. Mod. Phys. E **11**, 531 (2002).
- [21] R. Sahu and V.K.B. Kota, Phys. Rev. C **66**, 024301 (2002).
- [22] R. Sahu and V.K.B. Kota, Phys. Rev. C **67**, 054323 (2003).
- [23] S. Mishra, R. Sahu, and V.K.B. Kota, Prog. Theo. Phys. **118**, 59 (2007).
- [24] T.S. Kosmas, A. Faessler, and R. Sahu, Phys. Rev. C **68**, 054315 (2003).
- [25] R. Sahu, K.H. Bhatt, and D.P. Ahalpara, J. Phys. G **16**, 733 (1990).
- [26] R. Sahu, F. Šimkovic, and A. Faessler, J. Phys. G **25**, 1159 (1999).

- [27] S. Mishra, A. Shukla, R. Sahu, and V.K.B. Kota, Phys. Rev. C **78**, 024307 (2008).
- [28] A. Shukla, R. Sahu and V.K.B. Kota, Phys. Rev. C **80**, 057305 (2009).
- [29] R. Sahu and V.K.B. Kota, Int. J. Mod. Phys. E **20**, 1723 (2011).
- [30] R. Sahu, P.C. Srivastava and V.K.B. Kota, J. Phys. G **40**, 095107 (2013)
- [31] R. Sahu, P.C. Srivastava and V.K.B. Kota, Can. J. Phys. **89**, 1101 (2011)
- [32] J. Kotila and F. Iachello, Phys. Rev. C **87**, 024313 (2013).
- [33] J. Engel, P. Vogel and M. R. Zirnbauer, Phys. Rev. C **37**, 731-746 (1988)
- [34] T. Tomoda, Rep. Prog. Phys. **54**, 53-126 (1991).
- [35] F. Šimkovic, A. Faessler, H. Mütter, V. Rodin and M. Steuf, Phys. Rev. C **79**, 055501 (2009).
- [36] M. Horoi and S. Stoica, Phys. Rev. C **81**, 024321 (2010).
- [37] B.A. Brown and A.F. Lisetskiy (unpublished)
- [38] ENSDF Data Base, Brookhaven National Laboratory, USA, <http://www.nndc.bnl.gov/ensdf/index.jsp>.
- [39] D. von Ehrenstein and J.P. Schiffer, Phys. Rev. **164**, 1374 (1967).
- [40] V.K.B. Kota and V. Potbhare, Nucl. Phys. **A331**, 93 (1979).
- [41] J.P. Schiffer et. al., Phys. Rev. Lett. **108**, 022501 (2012).
- [42] J.P. Schiffer *et al.* Phys. Rev. Lett. **100**, 112501 (2008).
- [43] B.P. Kay et. al. Phys. Rev. C **79**, 021301(R) (2009).
- [44] F. Boehm and P. Vogel, *Physics of Massive Neutrinos* (Cambridge University Press, Cambridge, 1992).
- [45] G. Audi, A.H. Wapstra and C. Thibault, Nucl. Phys. **A729**, 337 (2003).
- [46] A. Bobyk et al. Nucl. Phys. A **669**, 221 (2000)
- [47] D.P. Ahalpara, K.H. Bhatt and R. Sahu, J. Phys. G **11**, 735 (1985)
- [48] S. Mishra, K.C. Tripathy and R. Sahu, Can. J. Phys. **85**, 269 (2007).
- [49] L. Simard J. Phys. Conf. Ser. **375**, 042011 (2012).
- [50] R.A. Sen'kov, M. Horoi and B.A. Brown, Phys. Rev. C **89**, 054304 (2014).
- [51] P.A.R. Ade *et al.* (Planck collaboration), arXiv:1303.5076; Astronomy and Astrophysics (in press).
- [52] P.S.B. Dev, S. Goswami, M. Mitra and W. Rodejohann, Phys. Rev. D **88**, 091301 (2013).

TABLE II: DSM model predicted $B(E2; J_i \rightarrow J_f)$ values in W.u. for ^{80}Kr and ^{82}Kr are compared with experimental data given in [38].

B(E2)'s for ^{80}Kr				B(E2)'s for ^{82}Kr			
J_i	J_f	DSM	Expt.	J_i	J_f	DSM	Expt.
2^+	0^+	23.1	37.3 ± 2.2	2^+	0^+	17.8	21.3 ± 0.7
$2'^+$	2^+	9.2	25 ± 5	$2'^+$	2^+	8.4	≈ 5.5
$2'^+$	0^+	2.1	0.30 ± 0.07	$2'^+$	0^+	2.6	
4^+	2^+	33.9	70 ± 10	$3'^+$	2^+	4.6	
$3'^+$	$2'^+$	38.4	34 ± 5	$3'^+$	$2'^+$	30.1	
$3'^+$	2^+	3.6	0.57 ± 0.14	4^+	2^+	25.5	32 ± 12
$4'^+$	4^+	7.2	32 ± 20	$4'^+$	$2'^+$	6.0	9 ± 3
$4'^+$	$2'^+$	11.0	50 ± 30	6^+	4^+	27.9	5.5 ± 1.9
$4'^+$	2^+	0.1	0.26 ± 0.18	$5'^+$	4^+	0.3	7.3 ± 2.1
6^+	4^+	38.8	62 ± 16	8^+	6^+	27.4	
$5'^+$	$3'^+$	19.5	50 ± 17	10^+	8^+	25.6	
$5'^+$	4^+	1.3	1.2 ± 0.7				
$6'^+$	6^+	4.1	17 ± 15				
$6'^+$	$4'^+$	20.2	33 ± 17				
$6'^+$	4^+	0.1	<0.23				
8^+	6^+	38.7	90^{+90}_{-45}				
10^+	8^+	11.1					

TABLE III: DSM results for half-lives for $0\nu\beta\beta$ with $m_\nu = 1$ eV (there are claims that the effective neutrino mass is certainly much less than 1 eV [51, 52]). The values of $G^{0\nu}$ given in column 2 are taken from Ref. [44]. Columns 3 and 4 are DSM results. Last column gives current experimental bounds for the half lives. See text for further details.

Nucleus	$G^{0\nu}(\text{yr}^{-1})$	$M^{0\nu}$	$T_{1/2}(\text{yr})$	Expt'l bound (yr)
^{70}Zn	0.23×10^{-26}	2.13	9.6×10^{25}	$\geq 3.2 \times 10^{19}$
^{80}Se	0.43×10^{-27}	3.48	1.9×10^{27}	— — —
^{82}Se	0.11×10^{-24}	2.16	1.9×10^{24}	$\geq 3.2 \times 10^{23}$

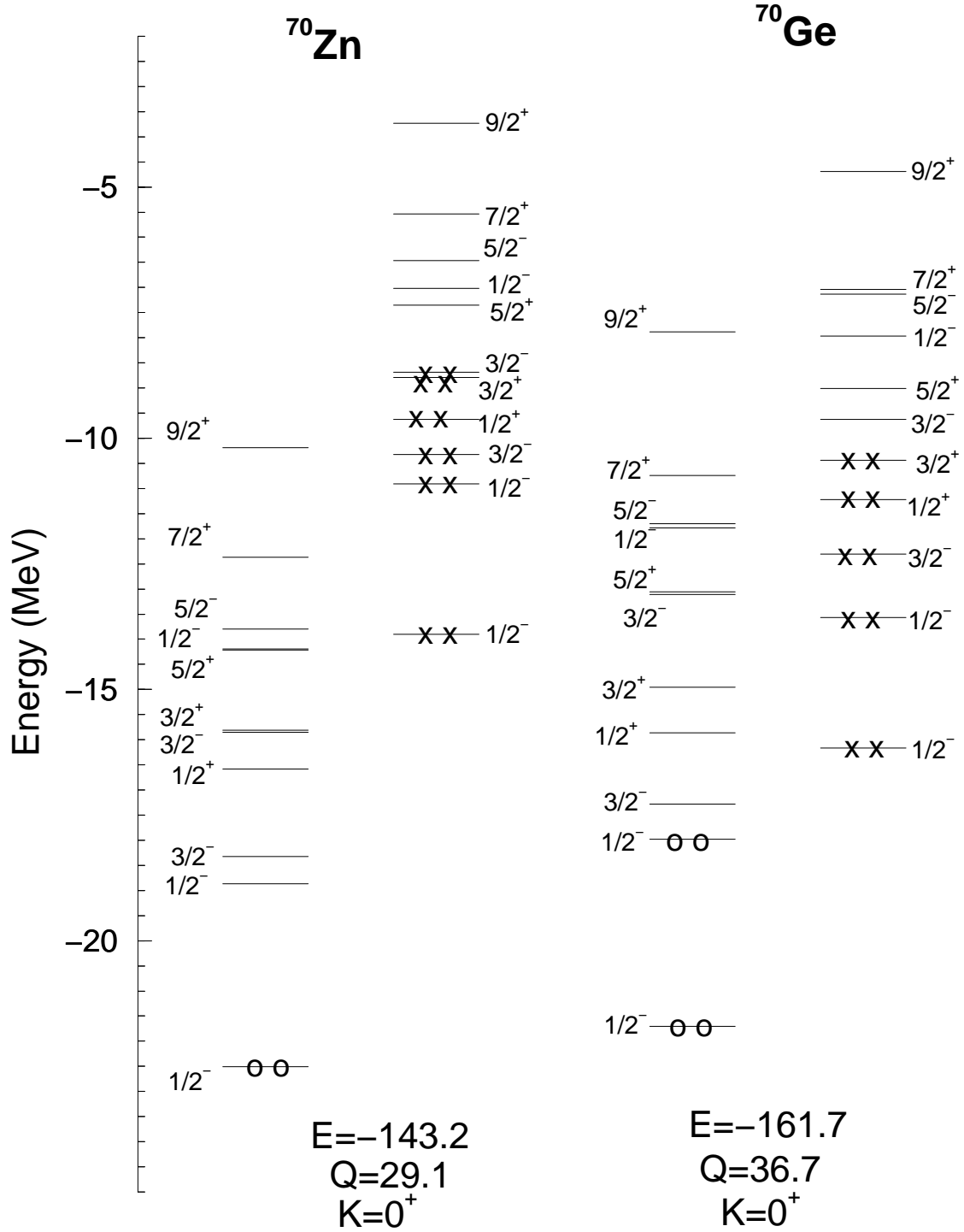


FIG. 1: HF single particle spectra for ^{70}Zn and ^{70}Ge corresponding to lowest prolate configurations. In the figures circles represent protons and crosses represent neutrons. The Hartree-Fock energy (E) in MeV, mass quadrupole moment (Q) in units of the square of the oscillator length parameter and the total K quantum number of the lowest intrinsic states are given in the figure. Each occupied single particle orbital is two fold degenerate because of time reversal symmetry.

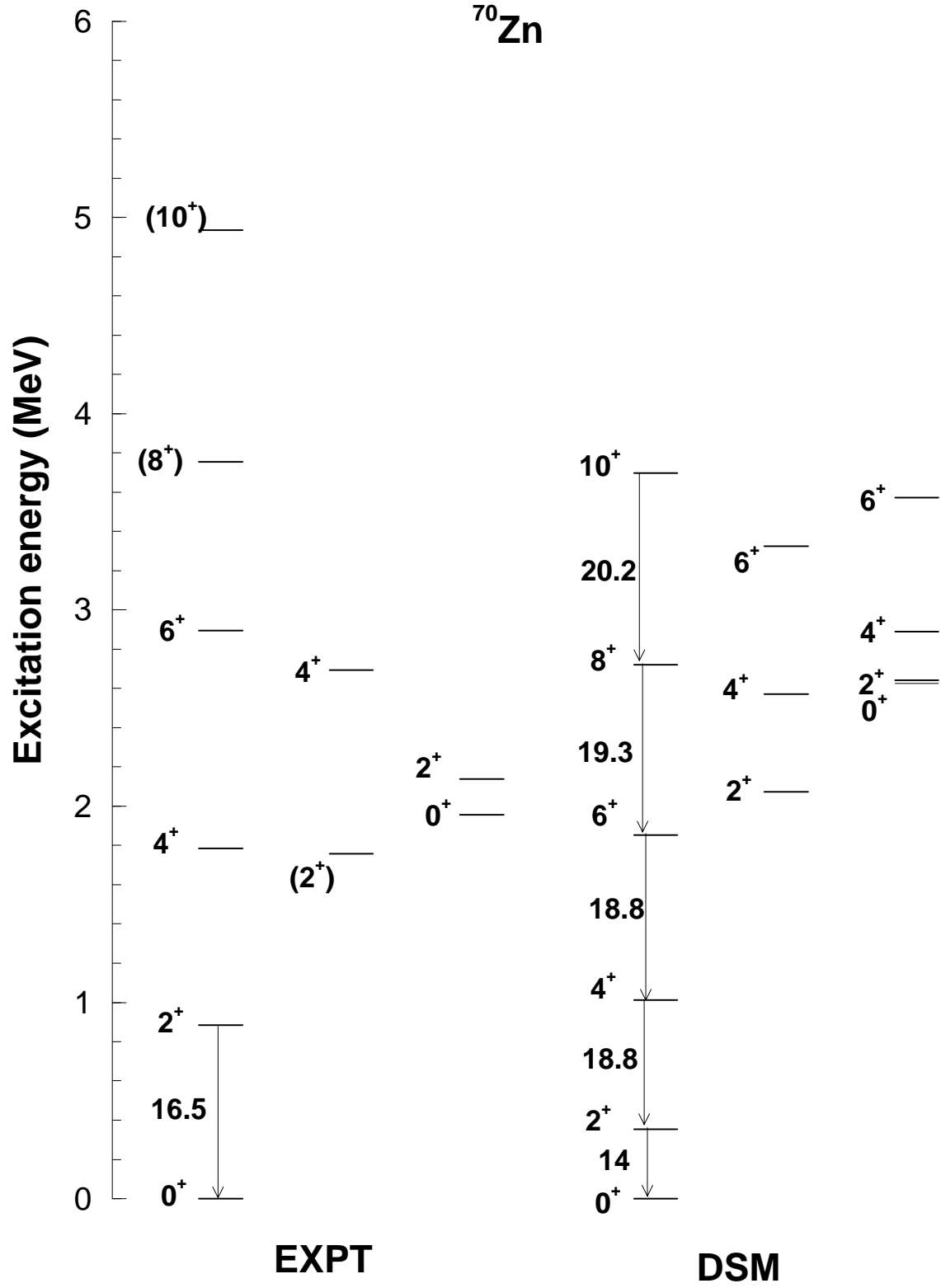


FIG. 2: The calculated energy levels for ^{70}Zn are compared with experiment. The experimental data are from ref [38]. The quantities near the arrows represent $B(E2)$ values in W.u.

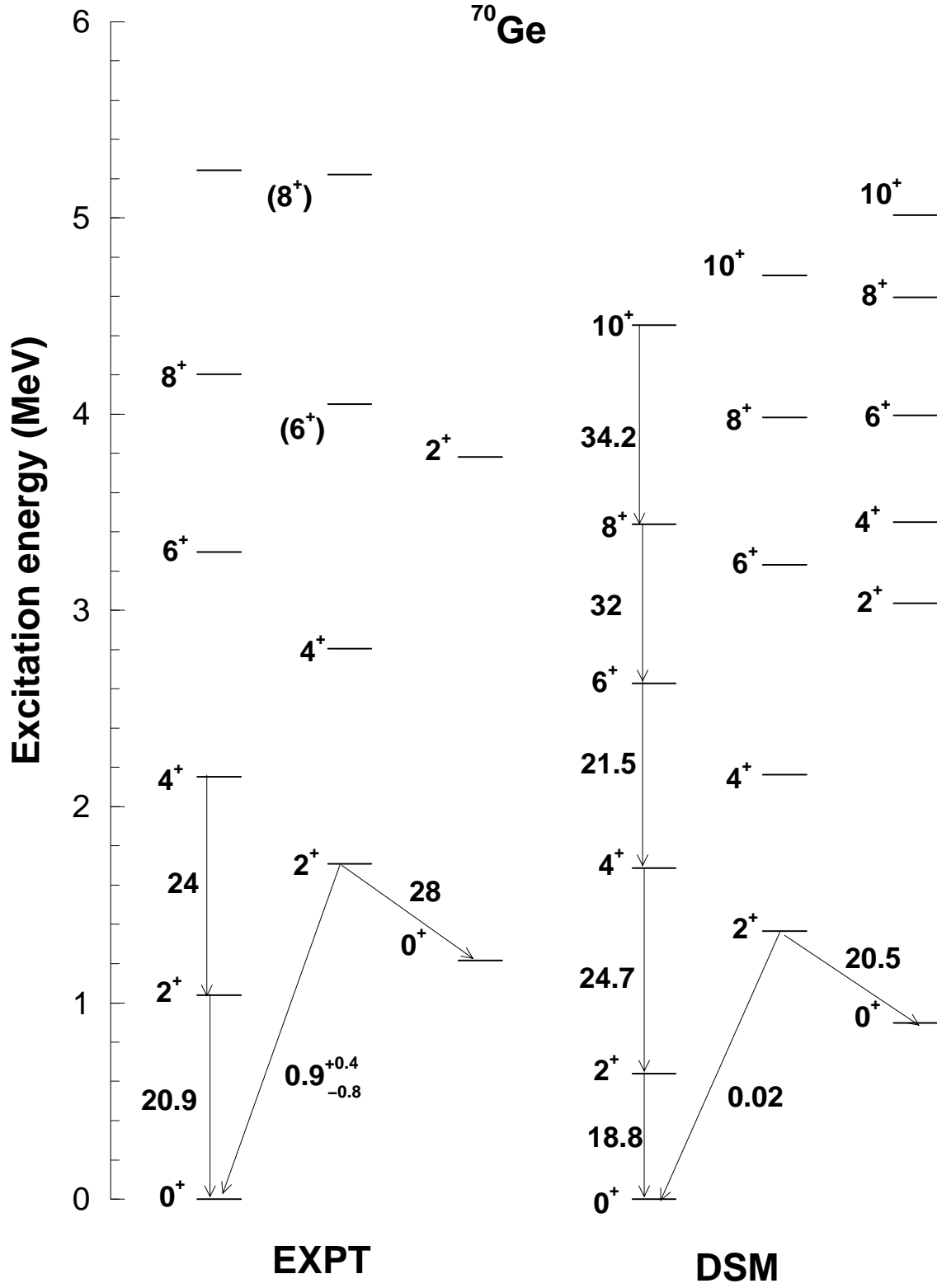


FIG. 3: The calculated energy levels for ^{70}Ge are compared with experiment. The experimental data are from ref [38]. The quantities near the arrows represent B(E2) values in W.u.

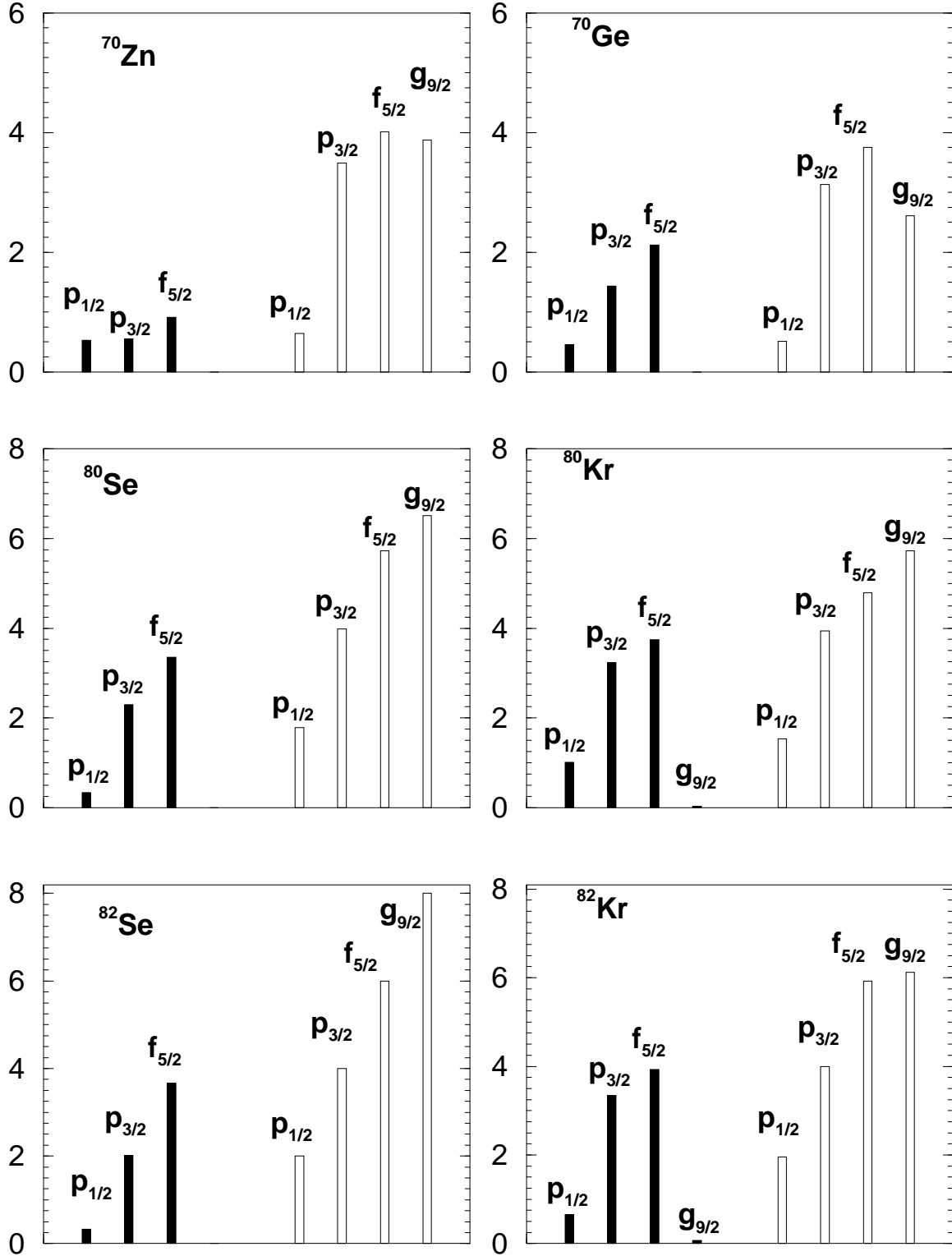


FIG. 4: DSM results for occupancies of different orbits. Filled bars are for proton occupancies and open bars are for neutron occupancies.

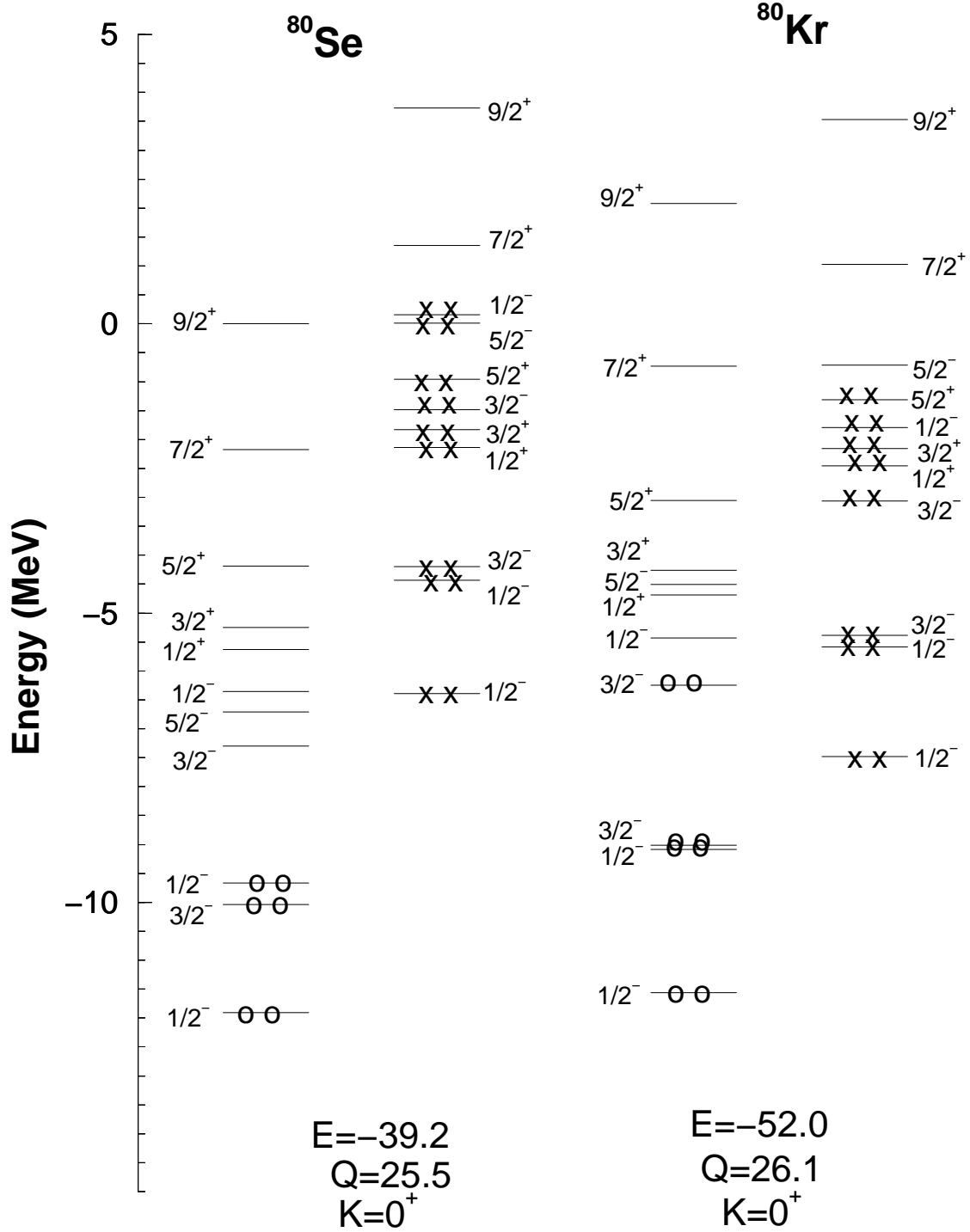


FIG. 5: HF single particle spectra for ^{80}Se and ^{80}Kr corresponding to lowest prolate configurations. In the figures circles represent protons and crosses represent neutrons. The Hartree-Fock energy (E) in MeV, mass quadrupole moment (Q) in units of the square of the oscillator length parameter and the total K quantum number of the lowest intrinsic states are given in the figure. Each occupied single particle orbital is two fold degenerate because of time reversal symmetry.

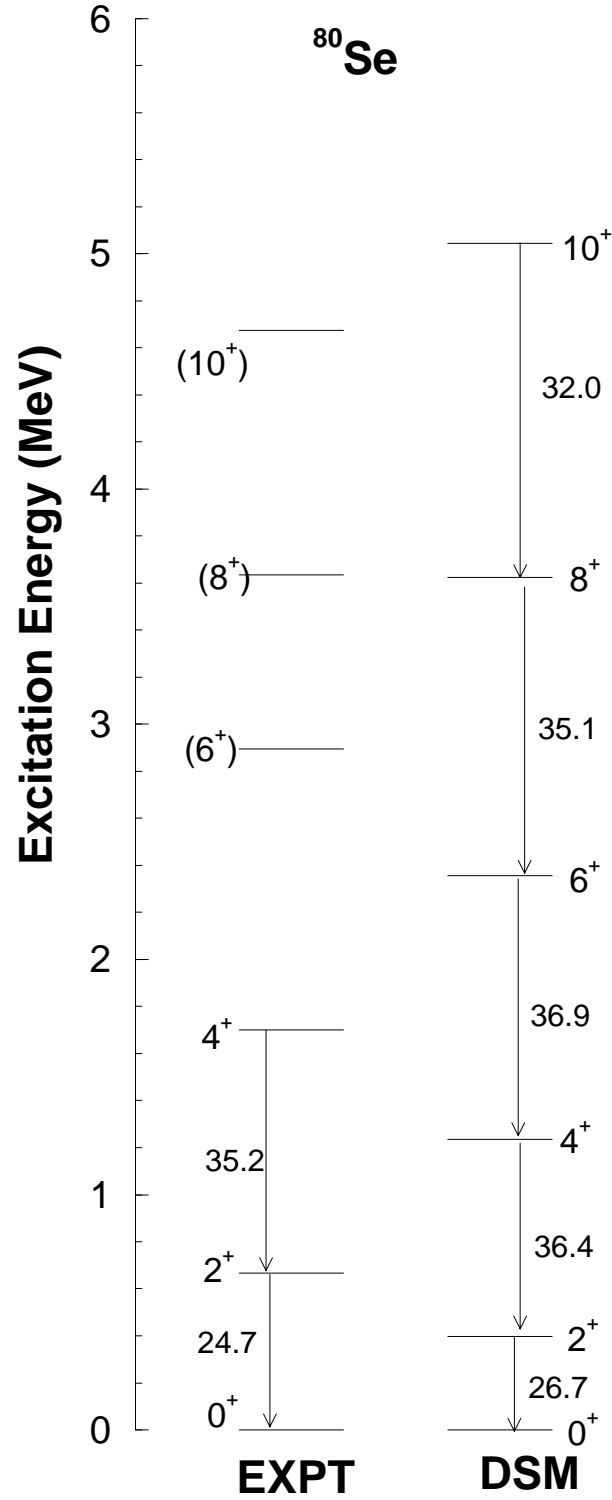


FIG. 6: The calculated energy levels for ^{80}Se are compared with experiment. The experimental data are from ref [38]. The quantities near the arrows represent $B(E2)$ values in W.u.

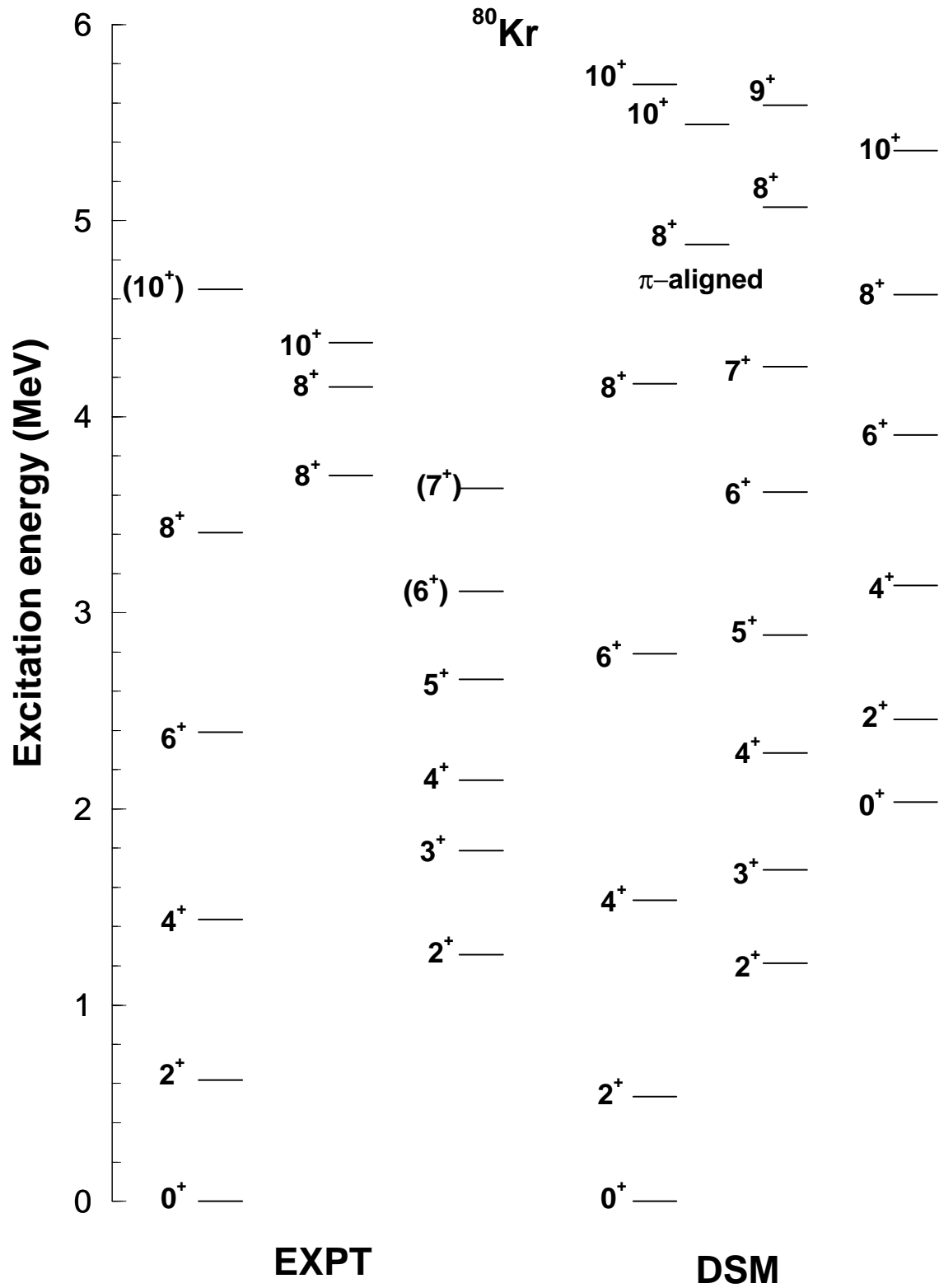


FIG. 7: The calculated energy levels for ^{80}Kr are compared with experiment. The experimental data are from ref [38].

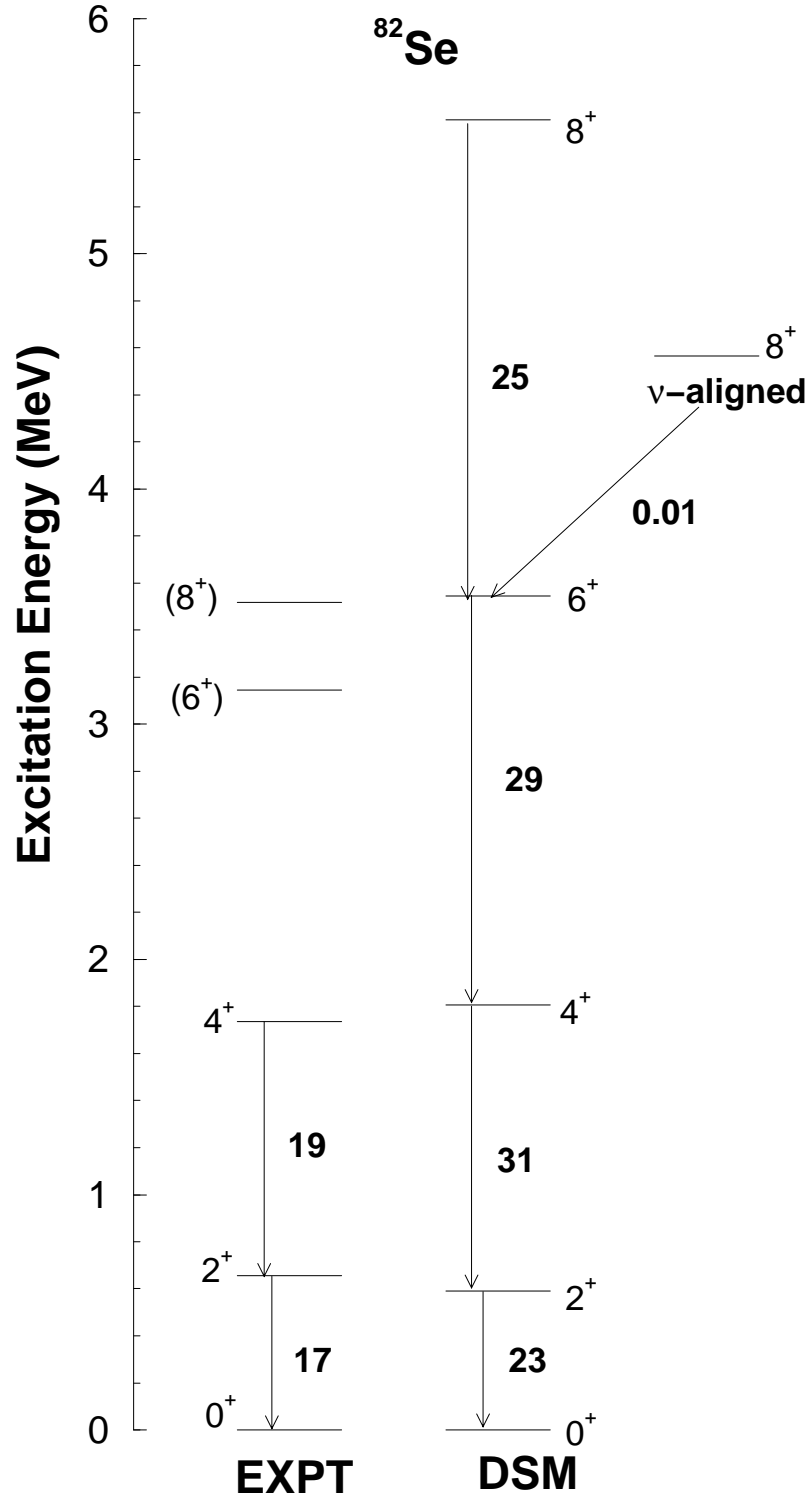


FIG. 9: The calculated energy levels for ^{82}Se are compared with experiment. The experimental data are from ref [38].

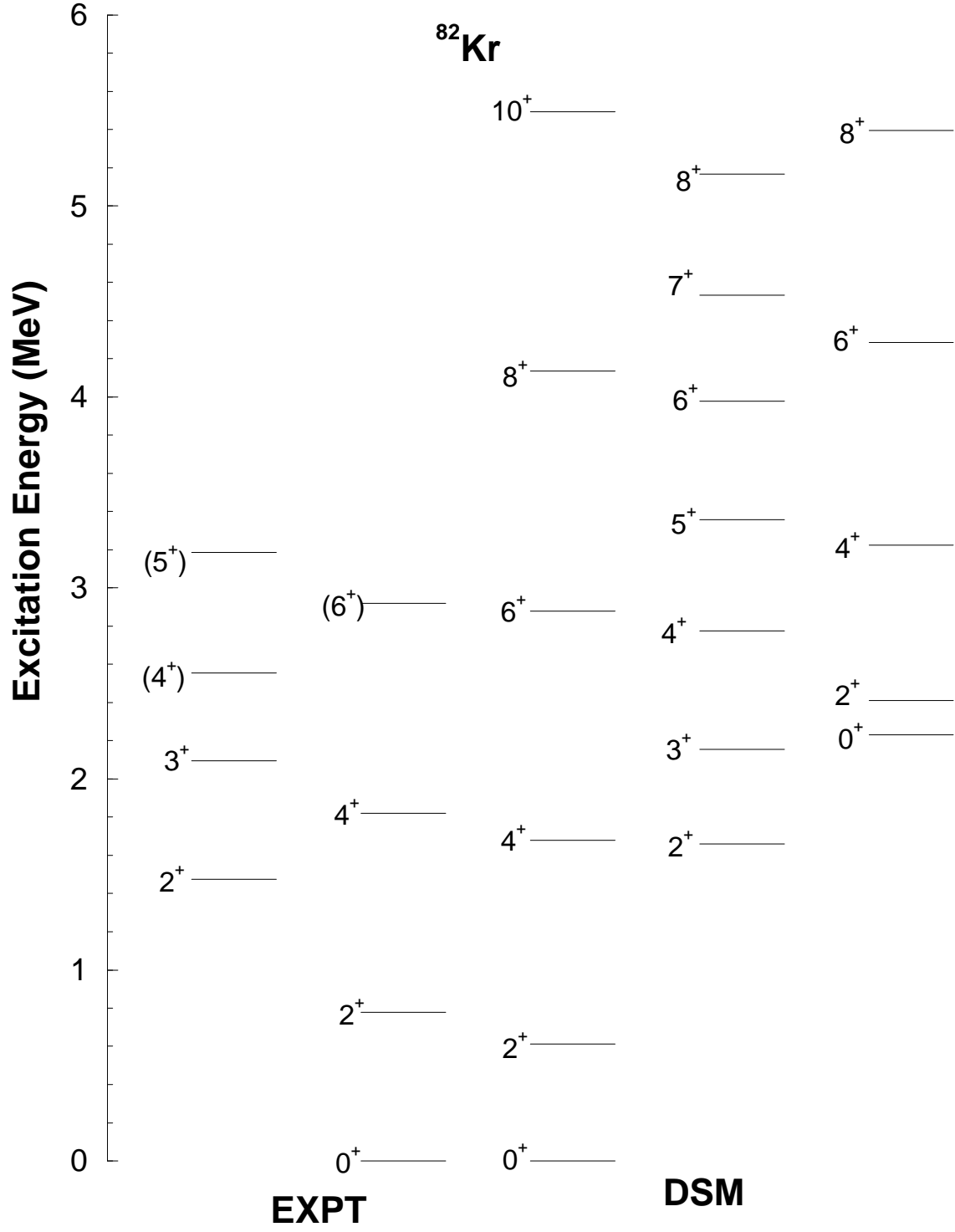


FIG. 10: The calculated energy levels for ^{82}Kr are compared with experiment. The experimental data are from ref [38].